PHYSICAL REVIEW B VOLUME 59, NUMBER 10 1 MARCH 1999-II

Origin of dispersive effects of the Raman *D* band in carbon materials

M. J. Matthews* and M. A. Pimenta†
Department of Physics, Massachusetts Institute of Technology, Cambridge, Massachusetts 02139

G. Dresselhaus
Francis Bitter Magnet Laboratory, Massachusetts Institute of Technology, Cambridge, Massachusetts 02139

M. S. Dresselhaus
Department of Physics and Department of Electrical Engineering and Computer Science, Massachusetts Institute of Technology, Cambridge, Massachusetts 02139

M. Endo
School of Engineering, Shinshu University, Nagano, 380 Japan
(Received 26 August 1998)

The origin and dispersion of the anomalous disorder-induced Raman band (*D* band) observed in all sp^2 hybridized disordered carbon materials near 1350 cm^{-1} is investigated as a function of incident laser energy. This effect is explained in terms of the coupling between electrons and phonons with the same wave vector near the *K* point of the Brillouin zone. The high dispersion is ascribed to the coupling between the optic phonons associated with the *D* band and the transverse acoustic branch. The large Raman cross section is due to the breathing motion of these particular phonons near the *K* point. Our model challenges the idea that the Raman *D* peak is due to laser-energy-independent features in the phonon density of states, but rather is due to a resonant Raman process. [S0163-1829(99)50410-4]

It has been known for almost 30 years that a modest amount of disorder can give rise to a band in the Raman spectrum of graphitic materials, which is not present in the Raman spectrum of single-crystal graphite.[1] This so-called disorder-induced band (or *D* band) occurs at about 1350 cm^{-1} for a laser excitation wavelength (λ_L) of 488 nm and its intensity (I_D) scales inversely with (graphitic) particle size. For a given λ_L, the intensity I_D can be quantitatively compared[2] to the intensity of the Raman-allowed E_{2g_2} mode (I_G) to yield the in-plane crystallite size L_a. Vidano *et al.*[3] performed a systematic investigation of the Raman spectra of different kinds of carbon materials by varying the laser excitation energy $\mathcal{E}_L$ (or the wavelength λ_L), and they observed that the frequency of this *D* band upshifts rapidly with increasing $\mathcal{E}_L$. It was also reported in this work that the frequency of the related overtone of the *D* band, the so-called second-order G' band (observed at about 2700 cm^{-1} using 488 nm laser excitation), also shifts with changing laser energy. The slope of the $\mathcal{E}_L$ dependence of the G' band frequency $\partial\omega/\partial\mathcal{E}_L$ was found to be approximately two times greater than that for the disorder-induced *D* band. Another important result reported by Vidano *et al.*[3] was that the second-order G' band exhibits a laser-dependent peak frequency even in the case of single-crystal graphite, where the disorder-induced *D* band is absent.

The same laser energy dependences of the *D* and G' Raman bands were found to occur in different kinds of carbon materials, such as graphon carbon black,[4] hydrogenated amorphous carbon,[5] glassy carbon and crystalline graphite,[6,7] multicomponent carbon films,[8] and carbon nanotubes,[9,10] and, in fact, these features are common to all kinds of carbon materials containing condensed aromatic structures.

Despite the fact that the presence of the *D* band and its laser energy dependence have been known for some time, and that the intensity of this band is commonly used for practical applications to evaluate the amount of disorder in carbon materials,[2] no detailed model has ever been proposed to explain the physical origin and the dispersion effect of the *D* band. In the model proposed by Tuinstra and Koenig[1] in 1970, the appearance of the *D* band was explained by considering the relaxation of the full D_{6h} symmetry for the case of finite graphite crystallites, thereby allowing many modes to show Raman activity. This model was later theoretically supported by a comprehensive molecular-orbital study of A_{1g} breathing modes in small aromatic clusters.[11] A closely related approach, which involves the general relaxation of symmetry, is the density-of-states (DOS) model,[12,13] which correlates features in the Raman spectrum of disordered carbons to features in the DOS.

However, both of the models described above fail to give an explanation of the observed dispersion of the *D* band with laser energy, which was first noted by Vidano *et al.*,[3] after the introduction of the two models described above. If the features in the Raman spectra of disordered carbons were simply due to DOS singularities, these features should not be dispersive. Some workers[14] have attributed the dispersion effect to selective sampling of various sized carbon clusters, in analogy with a similar effect observed in polyacetylene.[15,16] However, this selective sampling model cannot explain, in the limit of large crystallites ($L_a \rightarrow \infty$), the dispersion of the second-order band observed experimentally for ideal single-crystal graphite, which shows no disorder-induced scattering.

The first qualitative explanation for this effect was proposed by Baranov *et al.*,[6] who suggested that the dispersive

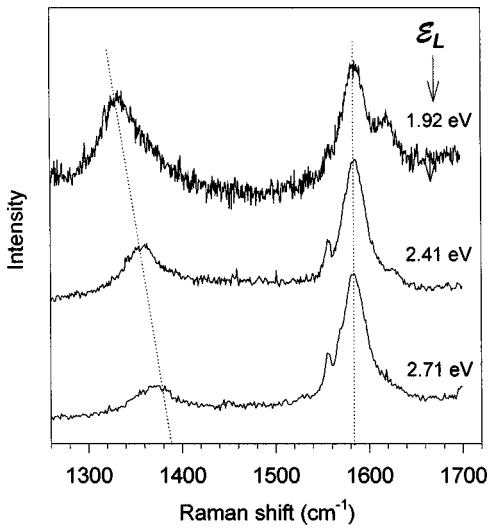

FIG. 1. Raman spectrum of PPP-2400 obtained with laser wavelengths 647 nm (1.92 eV), 514.5 nm (2.41 eV), and 457.9 nm (2.71 eV).

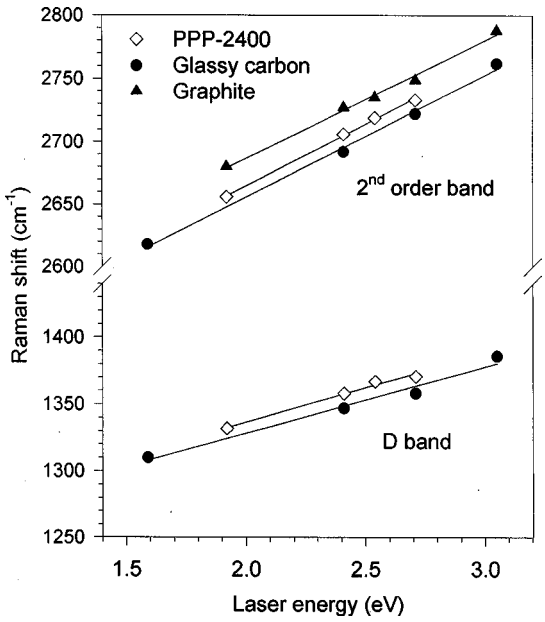

FIG. 2. Dependence of the frequencies of the *D* band and the second-order G' band on laser energy ($\mathcal{E}_L$) for PPP-2400 and glassy carbon (Ref. 7). Measurements on crystalline graphite (HOPG) are included for the second-order Raman band.

phonon frequencies were somehow due to selective coupling between phonons and electronic states having the same magnitude of the wave vector. According to this model, *all* phonon branches should contribute, which is not observed experimentally. We present here a model, which explains quantitatively the experimental Raman data and gives physical grounds for the dispersive behavior and for the large Raman cross-section of the particular phonon branch which gives rise to the disorder-induced *D* band and the related second-order G' band.

Because of the small variations in the mode frequencies for the *D* band from one sp^2-based carbon to another, we consider here *D*-band data for three different sp^2-based carbons: PPP-2400, which denotes polyparaphenylene (PPP) heat treated to a temperature of 2400 °C,[17] highly oriented pyrolytic graphite (HOPG), and glassy carbon.[7] Since PPP carbonizes in the temperature range 700−800 °C by the desorption of volatile species, the residue material after heat treatment to 2400 °C is a hard carbon which forms short graphene ribbons that are stacked with interplanar correlation lengths of only a few layers, based on x-ray-diffraction data.[18] Literature values for glassy carbon heat treated at 2000 °C were used for comparison. For the second-order spectra, measurements were made on PPP-2400 and on highly oriented pyrolytic graphite (HOPG), and literature values were used for glassy carbon.[7]

Raman-scattering experiments were performed at ambient conditions using a back-scattering geometry for the following laser excitation lines: krypton 647 nm (1.92 eV) and 407 nm (3.05 eV), and argon 514.5, 488, and 458 nm (2.41, 2.54, and 2.71 eV, respectively). The spectral resolution of the system was always better than 2 cm^{-1}. Figure 1 shows the Raman spectra of PPP-2400 obtained with three different laser excitation energies. Note that the position of the E_{2g_2} graphite band at 1580 cm^{-1} (the *G* band) does not depend on the laser energy $\mathcal{E}_L$, whereas the peak frequency of the *D* band near $\sim$1350 cm^{-1} increases with increasing laser energy. It is also interesting to observe in this figure that the ratio of the integrated intensities of the *D* and *G* bands (I_D/I_G) decreases with increasing laser energy $\mathcal{E}_L$.[19]

These facts have led to the misinterpretation[20] of the so-called Knight formula, $L_a = C(I_D/I_G)^{-1}$, where $C = 44$ Å. This value of the prefactor C is only applicable near $\lambda_L = 514.5$ nm, since C must depend on λ_L to accommodate for a λ_L-dependent intensity ratio $R(\lambda_L) = I_D/I_G$ such that $L_a = C(\lambda_L)/R(\lambda_L)$ where $C(\lambda_L)$ is a variable scaling coefficient. To estimate the appropriate $C(\lambda_L)$ for a given wavelength λ_L (in nm), we use the observation that for PPP-2400 and for all other available data on glassy carbons[6,7] and carbon blacks[4] heat treated above 2000 °C, R is linear in λ_L ($400 < \lambda_L < 700$ nm): $R(\lambda_L) \approx R_0 + \lambda_L R_1$. We can then estimate $C(\lambda_L)$ in the linear regime as $C(\lambda_L) \approx C_0 + \lambda_L C_1$, where C_0 and C_1 were estimated to be -126 Å and $C_1 = 0.033$, respectively, using $R(\lambda_L)$ data for PPP-2400.

In Fig. 2 we plot the laser energy ($\mathcal{E}_L$) dependence of the frequencies of the *D* band for PPP-2400 (see Fig. 1) and for glassy carbon, using data reported by Wang *et al.*[7] The *D*-band frequency ω vs $\mathcal{E}_L$ data can be well fit by straight lines. The slopes $\partial\omega/\partial\mathcal{E}_L$ are the same, $\partial\omega/\partial\mathcal{E}_L = 51$ cm^{-1}/eV, for the two sp^2 carbon materials in Fig. 2 and the intercepts are 1234 cm^{-1} for PPP-2400, and 1223 cm^{-1} for glassy carbon, respectively. The corresponding results for the second-order G' band are also plotted in Fig. 2 for PPP-2400, glassy carbon[7] and graphite. The fitting parameters of the linear regression for the slopes $\partial\omega/\partial\mathcal{E}_L$ for the second-order G' band show that the slopes for all three samples are the same, and are approximately two times the slope $\partial\omega/\partial\mathcal{E}_L$ for the *D* band, confirming that this second-order G' band is the second harmonic for the *D* band. It is interesting to note that although single-crystal graphite has no *D* band, it does have a G' band very similar to that of the disordered carbons. The variation in the *D*- and G'-band frequencies obtained with the same laser energy for the different carbon materials is ascribed to the slightly greater

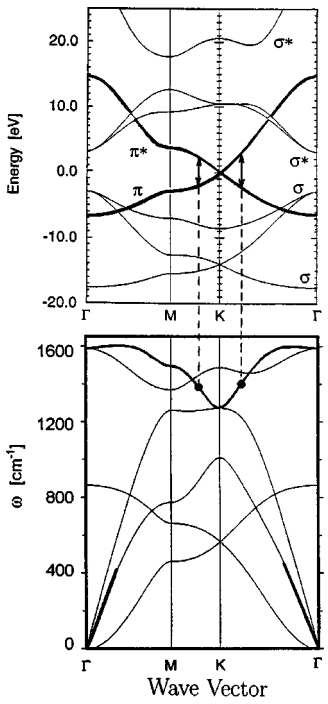

FIG. 3. Electronic energy bands of 2D graphite (top) (Refs. 21 and 22). Phonon dispersion curves of 2D graphite (bottom) (Refs. 21 and 22). Both the phonon branch that is strongly coupled to electronic bands in the optical excitation, and the electronic bands near the Fermi level ($E=0$) that are linear in k are indicated by heavy lines. The slope for the TA phonon branch is also indicated by heavy lines.

force constants for more well-ordered carbons. Therefore, the frequency of the second-order G' band for crystalline graphite is the highest among all carbon materials, as confirmed experimentally in Fig. 2. To explain the physical basis for our experimental results, let us start the discussion by comparing the electron and phonon dispersion curves for two-dimensional (2D) graphite.[21,22] We note in the electron dispersion curve in the upper part of Fig. 3, that electronic transitions between the π and π^* electronic states with energies corresponding to visible photons only occur in the vicinity of the *K* point in the Brillouin zone (BZ). Because of the linear k dispersion of the π and π^* bands near the *K* point, a resonance between the laser energy and the π-π^* electronic transition occurs at a different point $\vec{k}$ of the BZ for each laser energy $\mathcal{E}_L$, that is,

$$\mathcal{E}_L = \Delta E(\vec{k}) = E^c(\vec{k}) - E^v(\vec{k}), \tag{1}$$

where $\mathcal{E}_L$ is the incident laser energy and $E^{c,v}(\vec{k})$ are the electronic conduction or valence band energies. The π-electron dispersion near the *K* point in 2D graphite is nearly isotropic,[23] and because of the degeneracy of $E^c(\vec{k}_K)$ and $E^v(\vec{k}_K)$ at the *K* point, the energy difference ΔE between the valence and conduction bands can be written as

$$\Delta E(\Delta k) = E^c(\Delta k) - E^v(\Delta k) = \sqrt{3} a_0 \gamma_0 \Delta k, \tag{2}$$

where Δk is the distance between a given $\vec{k}$ point within the BZ and the *K* point ($\Delta\vec{k} = \vec{k}_K - \vec{k}$), while $\gamma_0 \sim 3.0$ eV is the nearest-neighbor C-C overlap energy, and a_0 is the in-plane graphite lattice constant (2.46 Å).

Baranov *et al.*[6] explained qualitatively the laser energy dependence of the *D*-band frequency by considering the optic phonon branch which produces the E_{2g_2} phonons at the Γ point. Recently Pocsik *et al.*[24] reported a similar explanation for this phenomena. This phonon branch is represented by the heavy curve in the phonon dispersion curves displayed in the lower part of Fig. 3. The phonons that are enhanced in the Raman process are those that have wavevectors Δq with the same magnitude as the wave-vectors Δk of the electronic transitions that are in resonance with the laser energy (see dashed line in Fig. 3). Because the coupling to phonons is strong when $\Delta k = \Delta q$, we can write $\mathcal{E}_L = \Delta E(\Delta k) = \sqrt{3} a_0 \gamma_0 \Delta q$.

Therefore, we can convert the experimental value for the slope $(\partial\omega/\partial\mathcal{E}_L)$ of the ω vs $\mathcal{E}_L$ data of Fig. 2 ($\partial\omega/\partial\mathcal{E}_L = 51$ cm^{-1}/eV) and write the slope of the *D*-band dispersion in a ω vs Δq plot as

$$\frac{\partial\omega}{\partial\Delta q} = \sqrt{3} a_0 \gamma_0 \frac{\partial\omega}{\partial\mathcal{E}_L} = 652 \text{ Å cm}^{-1}, \tag{3}$$

making use of the fact that $\Delta k = \Delta q$ for this process.

It is well known that the acoustic phonon branches in graphite are strongly coupled to the high frequency optic branches at the *K* point.[22,25] Therefore, there is a transfer of the high dispersivity of the acoustic branches in the long wavelength limit to the optic branches around the *K* point (see Fig. 3). Let us consider now the transverse-acoustic (TA) phonon branch which is also represented by a heavy line in the bottom of the phonon dispersion curves in Fig. 3. The group velocity v_{TA} of this acoustic phonon in the long wavelength limit is $v_{\mathrm{TA}} = 1.23 \times 10^4$ m/s $= 650$ Å cm^{-1},[23] very close to the value of $\partial\omega/\partial\Delta q$ shown in Eq. (3). This important result strongly suggests that the highly dispersive nature of the ''quasi-acoustic'' optic phonon branch close to the *K* point is due to the coupling between the optic and the transverse acoustic branches at the *K* point. This coupling is therefore responsible for the large frequency shift of the Raman *D* band observed in variable-laser-energy studies of disordered carbons. Since the velocity of the long wavelength TA phonon is isotropic in the basal plane of the graphite structure, the slope of the optic branch around and near the *K* point is also approximately isotropic, but with some spread as we move away from *K*-*M*. Therefore, it is reasonable to suppose that *all* the optic phonons of this branch that have the same magnitude Δq from the *K* point contribute to the *D* band and to the second-order G' band, in contrast to the conclusion of Baranov *et al.*[6] who considered only the phonons in the *K*-*M* direction. The contribution of *all* phonons around the *K* point can explain the large contribution of this optic branch to the *D*-band intensity, although the density of states for these phonons is not so large. The contributions from all the phonons around the *K* point also explain why these Raman bands tend to be broader than the Γ-point E_{2g_2} graphitic band around 1600 cm^{-1}.

A last question concerns the particularly large Raman cross section near the *K* point for the optic phonon branch shown in Fig. 3 as a heavy line. Eigenmode analysis shows

that the displacement of the atoms corresponding to the vibrational mode at the K point of this particular branch have a breathing-mode type behavior (e.g., see Fig. 5 of Ref. 1). In general, the modes which most strongly modulate the polarizability, and therefore have the largest Raman cross sections, are of a symmetric breathing type. Moreover, in a Franck-Condon analysis of the photoluminescence,[26] it is also this type of mode, which is considered to appear as a vibronic structure in the photoluminescence spectrum of most crystals or molecules, due to the very strong electron-phonon coupling. For this reason, this phonon branch makes the dominant contribution to the resonant Raman scattering process associated with the D band and the second order G'-band.

In summary, in this work we challenge the idea that the Raman D peak is due to laser-energy-independent features in the phonon density of states, but show rather that the peak is due to a resonant Raman process. The resonantly enhanced phonons are those that are at the same distance Δq from the K point as the electronic states at Δk that are in resonance with the laser energy, such that $\Delta q = \Delta k$. The optical phonon branch, which produces the E_{2g_2} phonons at the Γ point, appears to be mixed with the TA branch at the K point, and this is essential to understanding the highly dispersive nature of the Raman D band. The breathing character of these phonons explains their large cross section in a Raman scattering experiment.

The authors are thankful to Professor R. A. Jishi and Professor R. Saito for useful discussions. One of us (M.A.P.) is thankful to the Brazilian agency CAPES for financial support during his visit to MIT. The authors acknowledge support for this work under NSF Grant No. DMR 98-04734. The measurements performed at the George R. Harrison Spectroscopy Laboratory at MIT were supported by the NIH Grant No. P41-RR02594 and NSF Grant No. CHE9708265.

*Present address: Lucent Technologies, Room 1A-361, Murray Hill, NJ 07974; electronic address: mjmatthews@lucent.com

†Permanent address: Departamento de Fisica, Universidade Federal de Minas Gerais, Belo Horizonte, 30123-970 Brazil; electronic address: mpimenta@fisica.ufmg.br

[1] F. Tuinstra and J. L. Koenig, J. Chem. Phys. **53**, 1126 (1970).

[2] D. S. Knight and W. B. White, J. Mater. Res. **4**, 385 (1989).

[3] R. P. Vidano, D. B. Fishbach, L. J. Willis, and T. M. Loehr, Solid State Commun. **39**, 341 (1981).

[4] T. P. Mernagh, R. P. Cooney, and R. A. Johnson, Carbon **22**, 39 (1984).

[5] M. Ramsteiner and J. Wagner, Appl. Phys. Lett. **51**, 1355 (1987).

[6] A. V. Baranov, A. N. Bekhterev, Y. S. Bobovich, and V. I. Petrov, Opt. Spektrosk. **62**, 612 (1987).

[7] Y. Wang, D. C. Alsmeyer, and R. L. McCreery, Chem. Mater. **2**, 557 (1990).

[8] B. Marcus, L. Fayette, M. Mermoux, L. Abello, and G. Lucazeau, J. Appl. Phys. **76**, 3463 (1994).

[9] J. Kastner, T. Pichler, H. Kuzmany, S. Curran, W. Blau, D. N. Weldon, M. Dlamesiere, S. Draper, and H. Zandbergen, Chem. Phys. Lett. **221**, 53 (1994).

[10] A. M. Rao, E. Richter, S. Bandow, B. Chase, P. C. Eklund, K. W. Williams, M. Menon, K. R. Subbaswamy, A. Thess, R. E. Smalley, G. Dresselhaus, and M. S. Dresselhaus, Science **275**, 187 (1997).

[11] K. Yoshizawa, K. Okahara, T. Sato, K. Tanaka, and T. Yamabe, Carbon **32**, 1517 (1994).

[12] R. J. Nemanich and S. A. Solin, Phys. Rev. B **20**, 392 (1979).

[13] P. Lespade, R. Al-Jishi, and M. S. Dresselhaus, Carbon **20**, 427 (1982).

[14] M. Yoshikawa, G. Katagiri, H. Ishida, A. Ishitani, and T. Akamatsu, Solid State Commun. **66**, 1177 (1988).

[15] I. Harada, M. Tasumi, H. Shirakawa, and S. Ikeda, Chem. Lett. **1978**, 1411.

[16] E. Mulazzi, G. P. Brivio, E. Faulques, and S. Lefrant, Solid State Commun. **46**, 851 (1983).

[17] M. A. Pimenta, A. Marucci, and M. S. Dresselhaus (unpublished).

[18] M. Endo, C. Kim, T. Hiraoka, T. Karaki, K. Nishimura, M. J. Matthews, S. D. M. Brown, and M. S. Dresselhaus, J. Mater. Res. **13**, 2023–2030 (1998).

[19] K. Sinha and J. Menendez, Phys. Rev. B **41**, 10 845 (1990).

[20] L. Nikiel and P. W. Jagodzinski, Carbon **31**, 1313 (1993).

[21] R. Saito, G. Dresselhaus, and M. S. Dresselhaus, *Physical Properties of Carbon Nanotubes* (Imperial College Press, London, 1998).

[22] R. A. Jishi, L. Venkataraman, M. S. Dresselhaus, and G. Dresselhaus, Chem. Phys. Lett. **209**, 77–82 (1993).

[23] B. T. Kelly, *Physics of Graphite* (Applied Science, London, 1981).

[24] I. Pocsik, M. Hundhausen, M. Koos, and L. Ley, J. Non-Cryst. Solids **227-230B**, 1083 (1998).

[25] R. Al-Jishi and G. Dresselhaus, Phys. Rev. B **26**, 4514 (1982).

[26] M. J. Matthews, S. D. M. Brown, M. S. Dresselhaus, M. Endo, T. Takamuku, and Y. Karaki, J. Mater. Res. (to be published March 1999).